Civil Engineering Infrastructures Journal, 52(2): 309 – 322, December 2019
Print ISSN: 2322-2093; Online ISSN: 2423-6691
DOI: 10.22059/ceij.2019.267227.1517

Refinement to the Existing Analytical Methods of Analysis of Buried Pipelines due to Strike-Slip Faulting

Sabermahany, H.[1] and Bastami, M.[2*]

[1] Ph.D. Student in Earthquake Engineering, School of Civil Engineering, College of Engineering, University of Tehran, Tehran, Iran.
[2] Associate Professor of Department of Structure, International Institute of Earthquake Engineering and Seismology (IIEES), Tehran, Iran.

Received: 10 Oct. 2018; Revised: 03 Oct. 2019; Accepted: 06 Oct. 2019

ABSTRACT: Analytical methods presented to analyze the buried steel pipelines at strike-slip fault crossing use the Euler-Bernoulli beam theory. The cross-section of a buried pipe that is completely surrounded by soil cannot rotate freely and would not be remained perpendicular to the bending line after deformation. So it would be better to take into consideration a rotation between the cross-section and the bending line. The developed model improves the existing methodologies by using the Timoshenko beam theory and considering the shear deformations as a refinement to the existing methodologies. The proposed model results are compared with the results of an existing analytical model and it is found that the maximum bending and axial strains decrease with taking into consideration the shear deformations. Furthermore, it is shown that the difference between the results of models increases with an increase in the burial depth.

Keywords: Buried Steel Pipelines, Stress-Strain Analysis, Strike-Slip Fault Crossing, Structural Design Of Pipelines, Timoshenko Beam Theory.

INTRODUCTION

Buried pipelines carry essential resources for human life like water, natural gas and petroleum products, so they are referred to as "lifelines''. Analysis of buried pipelines for fault movement is important in their seismic design because of two considerable reasons. First, it is likely that buried pipelines cross active faults due to their huge length. Second, the break of the pipeline at one location disrupts its function completely. Significant damages in water and gas buried pipelines because of fault crossings were reported in past earthquakes (O'Rourke and Palmer, 1996; Towhata, 2010; O'Rourke and Liu, 2012).

Analysis of buried pipelines due to fault movement has been investigated analytically and numerically. As the first research, Newmark and Hall (1975) were developed a model for the fault crossing problem. It was assumed that the pipe deforms like a cable. This assumption confines the usage of the model for the case where the fault intersection angle is such that the pipe will be mainly exposed to tensile strains. An extended model of Newmark and Hall model which considered lateral soil-pipe interaction was carried out by Kennedy et al. (1977).

* Corresponding author E-mail: m.bastami@iiees.ac.ir

Wang and Yeh (1985) investigated a closed-form analytical model. The pipeline-soil system was considered by virtue of beams on elastic foundation theory. They also included the pipe bending stiffness in their model. This model was further improved by Karamitros et al. (2007). Both transverse and axial pipe-soil interaction were considered and the stress-strain relationship was assumed bilinear in order to take into account the material nonlinearity. Trifonov and Cherniy (2010) recommended some refinements to the previous methodology. They did not use the symmetry condition and also took into account the elongation caused by pipe bending. Furthermore, Sarvanis and Karamanos (2017) presented an analytical methodology for analysis of buried pipelines due to ground-induced deformations. The presented methodology, which was based on the assumption of a particular shape function for pipeline deformation, led to expressions for the maximum strain generated in the pipeline. Also, an equivalent static model was used to determine the length of the deformed pipeline shape.

Takada et al. (2001) presented a hybrid beam-shell finite element model to determine the maximum strain induced in pipes due to fault movement. The pipe was assumed to deform according to a bent deformation near the fault and then the maximum strain was obtained with regard to the bent angle. Xie et al. (2011) considered a 1-D beam finite element model alongside with a 3-D shell finite element model to obtain the bending and axial strains generated in HDPE pipes exposed to strike-slip fault crossing. Good agreement between the results of finite element analysis employing pipe beam elements with a modified bilinear soil spring model and the results of a series of physical tests was obtained. The modified bilinear soil spring model was developed via the results of tactile pressure sensors which were used in the physical tests to monitor the pressure at the soil-pipe interface. All the mentioned studies up to this point considered continuous buried pipelines and segmented pipelines were not specially considered. Xie et al. (2013) considered the numerical modeling of HDPE pipes exposed to normal fault crossing similar to the previous study. Erami et al. (2015) studied the applicability of pipe-soil interaction equations presented in pipeline seismic design codes to segmented pipelines. It was shown that the mechanical connection joints affect the performance of segmented pipelines due to faulting. The results of this study indicated the effect of the nature of soil behavior on the soil-pipe interaction equations and new pipe-soil interaction equations for segmented pipelines were developed.

The numerical stress-strain analysis of buried steel pipelines subjected to strike-slip faulting was also performed via the finite element method in some other studies (Chaudhari et al., 2013; Demofonti et al., 2013; Zhang et al., 2014, 2016; Trifonov, 2015; Uckan et al., 2015; Vazouras et al., 2015). Moreover, behavior of buried pipeline due to normal, reverse and strike-slip faulting was considered in some studies experimentally (Ha et al., 2010; Abdoun et al., 2009; Moradi et al., 2013; Hojat Jalali et al., 2016, 2018; Saiyar et al., 2016; Van Es and Gresnigt, 2016; Sarvanis et al., 2017).

In this paper, a solution for the stress-strain analysis of buried steel pipelines subjected to strike-slip fault movement is investigated by following the general concepts employed in the Karamitros et al. (2007) methodology. The Timoshenko beam theory is used in the proposed model to consider the shear deformations. Some researchers used the Timoshenko beam to model buried pipes in past studies (Barros and Pereira, 2004; Rashidifar and Rashidifar, 2013). In the buried pipelines that pipe is completely surrounded by soil, the soil deformation affects the buried pipe deformation and the

cross-section cannot rotate freely and would not be remained perpendicular to the bending line. So it would be better to take into account a rotation between the cross-section and the bending line that comes from the shear deformations. Following the Karamitros et al. (2007) model, the pipeline is divided into four segments and these segments are analyzed according to the Timoshenko beam on elastic foundation and the Timoshenko beam theory. The proposed model results indicate that the bending and axial strains decrease with taking into consideration the shear deformations. Moreover, it is shown that the difference between the results of the proposed model and the model introduced by Karamitros et al. (2007) increases when the burial depth is greater.

METHODOLOGY OUTLINE

Pipeline Model

Figure 1 indicates the pipeline which is divided into four segments by following the Karamitros et al. (2007) model and also shows the coordinate system of each segment. Point B is the fault crossing point.

Analyzing Segments AA′ and CC′

Segments AA′ and CC′ (see Figure 1) are analyzed as the Timoshenko beam on elastic foundation. The governing ordinary differential equations are (Yin, 2000):

$$D_1 \frac{d^2\psi}{dx^2} - C_1\psi + C_1 \frac{dw}{dx} = 0 \quad (1)$$

$$C_1 \frac{d\psi}{dx} - C_1 \frac{d^2w}{dx^2} + k_s w = 0 \quad (2)$$

where the transverse horizontal displacement (w) and the rotation angle (ψ) are two independent variables, k_s: is the transverse horizontal soil springs constant and D_1, C_1: are the bending and the shear stiffness, respectively, which can be expressed as:

$$D_1 = E_1 I \quad (3)$$

$$C_1 = kG_1A_s \quad (4)$$

where E_1: is the elastic Young's modulus of the pipeline steel, I: is the moment of inertia of the pipeline cross-section, G_1: is the shear modulus, A_s: is the area of the pipeline cross-section and k: is the shear coefficient factor which is calculated for hollow circular cross-section by (Hutchinson, 2001):

$$k = \frac{6\left(r^2+R^2\right)^2\left(1+\nu\right)^2}{7r^4+34r^2R^2+7R^4+\nu\left(12r^4+48r^2R^2+12R^4\right)+\nu^2\left(4r^4+16r^2R^2+4R^4\right)} \quad (5)$$

where R: is the outer radius and r: is the inner radius. Also, ν: is Poisson's ratio.

Eqs. (1) and (2) can be reduced to (see the Appendix):

$$D_1 \frac{d^4w}{dx^4} - \frac{k_s D_1}{C_1}\frac{d^2w}{dx^2} + k_s w = 0 \quad (6)$$

The solution of Eq. (6) takes the form (Yin, 2000):

$$w = e^{\alpha x}(c_1\cos\beta x + c_2\sin\beta x) + e^{-\alpha x}(c_3\cos\beta x + c_4\sin\beta x) \quad (7)$$

where

$$\alpha = \sqrt{\sqrt{\frac{k_s}{4D_1}} + \frac{k_s}{4C_1}} \text{ and } \beta = \sqrt{\sqrt{\frac{k_s}{4D_1}} - \frac{k_s}{4C_1}} \text{ for } k_s \prec \frac{4C_1^2}{D_1} \quad (8)$$

Imposing the boundary conditions, $w = 0$ for $x = 0$ and $w \to 0$ for $x \to \infty$ (points A′ and C′ are at a distance from A and C that transverse displacements are attenuated), Eq. (7) yields:

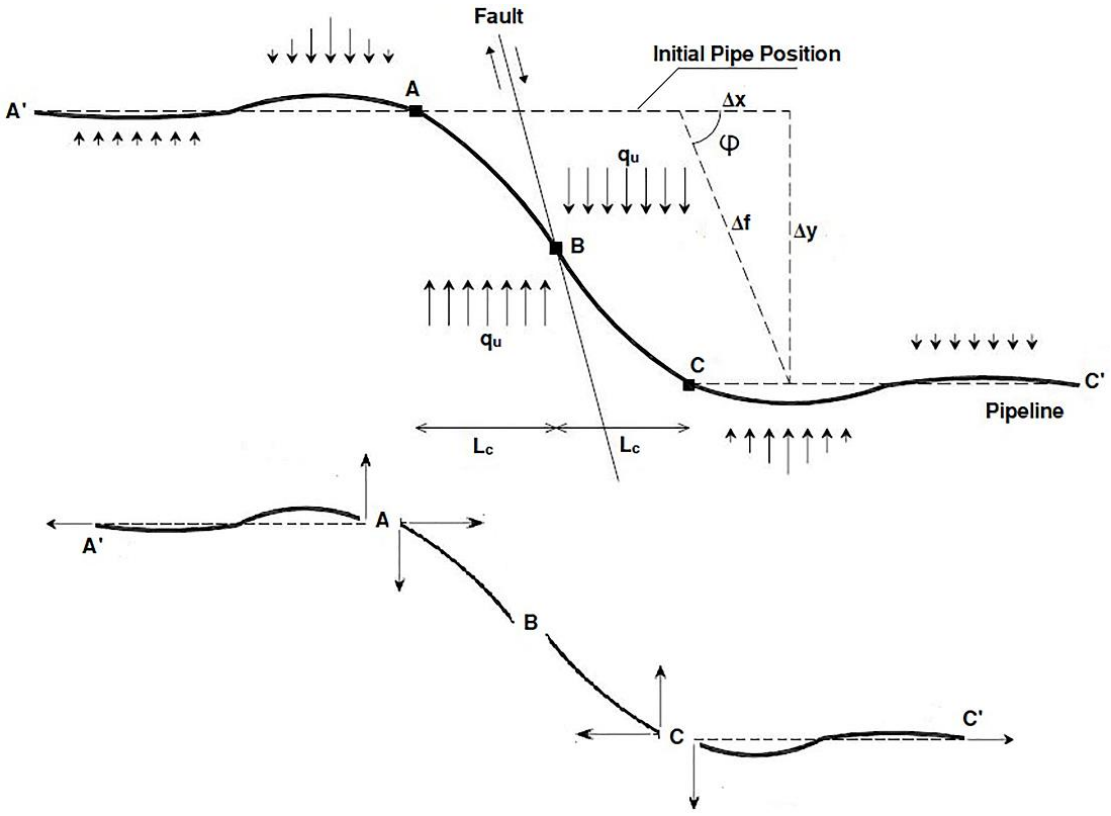

Fig. 1. Partitioning of the pipeline into four segments by following the Karamitros et al. (2007) model

$$w = e^{-\alpha x} c_4 \sin \beta x = A e^{-\alpha x} \sin \beta x \tag{9}$$

The bending moment (M) and the shear force (V) in the Timoshenko beam are given by (Timoshenko, 1921):

$$M = -D_1 \frac{d\psi}{dx} \tag{10}$$

$$V = C_1 \gamma = C_1 \left(\frac{dw}{dx} - \psi \right) \tag{11}$$

By using Eqs. (1), (2) and (9), the following relations are obtained:

$$\frac{d\psi}{dx} = \frac{d^2 w}{dx^2} - \frac{k_s w}{C_1} \tag{12}$$

$$C_1 \left(\frac{dw}{dx} - \psi \right) = -D_1 \frac{d^2 \psi}{dx^2} \tag{13}$$

$$\psi = \frac{dw}{dx} + \frac{D_1}{C_1} \frac{d^2 \psi}{dx^2} \tag{14}$$

$$\frac{dw}{dx} = A e^{-\alpha x} \left(-\alpha \sin \beta x + \beta \cos \beta x \right) \tag{15}$$

$$\frac{d^2 w}{dx^2} = A e^{-\alpha x} \left[\left(\alpha^2 - \beta^2 \right) \sin \beta x - 2\alpha\beta \cos \beta x \right] \tag{16}$$

$$\frac{d\psi}{dx} = \frac{d^2 w}{dx^2} - \frac{k_s w}{C_1} = A e^{-\alpha x} \left[\left(\alpha^2 - \beta^2 \right) \sin \beta x - 2\alpha\beta \cos \beta x \right] - \frac{A k_s}{C_1} e^{-\alpha x} \sin \beta x \tag{17}$$

$$\frac{d^2 \psi}{dx^2} = \frac{d}{dx} \left(\frac{d\psi}{dx} \right) = -A\alpha e^{-\alpha x} \left[\left(\alpha^2 - \beta^2 \right) \sin \beta x - 2\alpha\beta \cos \beta x \right] + A e^{-\alpha x} \left[\beta \left(\alpha^2 - \beta^2 \right) \cos \beta x + 2\alpha\beta^2 \sin \beta x \right] + \frac{A\alpha k_s}{C_1} e^{-\alpha x} \sin \beta x - \frac{A\beta k_s}{C_1} e^{-\alpha x} \cos \beta x \tag{18}$$

Now the bending moment, the shear force and the rotation angle for point A are determined:

$$M_{\mathrm{A}} = M\big|_{x=0} = -D_1 \frac{d\psi}{dx}\Big|_{x=0} = -D_1 \times -2A\alpha\beta = 2A\alpha\beta D_1 \tag{19}$$

$$V_{\mathrm{A}} = V\big|_{x=0} = C_1\left(\frac{dw}{dx} - \psi\right)\Big|_{x=0} = -D_1 \frac{d^2\psi}{dx^2}\Big|_{x=0} = -D_1 \times \left[2A\alpha^2\beta + A\alpha^2\beta - A\beta^3 - \frac{A\beta k_{\mathrm{s}}}{C_1}\right] = AD_1\beta\left[-3\alpha^2 + \beta^2 + \frac{k_{\mathrm{s}}}{C_1}\right] \tag{20}$$

$$\psi_{\mathrm{A}} = \psi\big|_{x=0} = \frac{dw}{dx}\Big|_{x=0} + \frac{D_1}{C_1}\frac{d^2\psi}{dx^2}\Big|_{x=0} = A\beta + \frac{AD_1\beta}{C_1}\left[3\alpha^2 - \beta^2 - \frac{k_{\mathrm{s}}}{C_1}\right] \tag{21}$$

Analogous relations apply for point C due to symmetry.

Analyzing Segments AB and BC

For segment AB or BC, the pipe-soil interaction is considered equal to a uniformly distributed load (q_{u}). The intensity of the distributed load (q_{u}) is equal to the maximum lateral soil force per unit length of the pipe (P_{u}) which is expressed in cohesionless soil (sand) as (ALA-ASCE, 2001):

$$q_{\mathrm{u}} = P_{\mathrm{u}} = N_{\mathrm{qh}}\gamma H(2R) \tag{22}$$

where N_{qh}: is the horizontal bearing capacity factor, γ: is the effective unit weight of the soil and H: is the depth of the soil. The expression for N_{qh} is (ALA-ASCE, 2001):

$$N_{\mathrm{qh}} = a + b\left(\frac{H}{2R}\right) + c\left(\frac{H}{2R}\right)^2 + d\left(\frac{H}{2R}\right)^3 + e\left(\frac{H}{2R}\right)^4 \tag{23}$$

where a, b, c, d and e: are defined in the ALA-ASCE guidelines (2001).

By using the Timoshenko beam theory, the equilibrium equations of segment AB are as follows:

$$D\frac{d^2\psi}{dx^2} - C\psi + C\frac{dw}{dx} = 0 \tag{24}$$

$$C\frac{d\psi}{dx} - C\frac{d^2w}{dx^2} = q \tag{25}$$

where

$$D = EI \tag{26}$$

$$C = kGA_{\mathrm{s}} \tag{27}$$

where E: is Young's modulus of the pipeline steel (for the analysis of segments AB and BC where the maximum bending moment occurs, the secant Young's modulus is used). Combining two equilibrium equations leads to (see the Appendix):

$$D\frac{d^4w}{dx^4} = q - \frac{D}{C}\frac{d^2q}{dx^2} \tag{28}$$

As mentioned before, q is constant for the segment AB or BC and equal to q_{u}. So the equilibrium equation is obtained as:

$$D\frac{d^4w}{dx^4} = q_{\mathrm{u}} \tag{29}$$

The solution of Eq. (29) is determined as:

$$w = a_0x^4 + a_1x^3 + a_2x^2 + a_3x + a_4 \tag{30}$$

and

$$w\big|_{x=0} = 0 \Rightarrow a_4 = 0 \tag{31}$$

$$\frac{d^4w}{dx^4} = 24a_0 \Rightarrow 24a_0D = q_{\mathrm{u}} \Rightarrow a_0 = \frac{q_{\mathrm{u}}}{24D} \tag{32}$$

By using Eqs. (24), (25) and (30), the following relations are determined:

$$\frac{d\psi}{dx}=\frac{d^2w}{dx^2}+\frac{q_u}{C}=12a_0x^2 \\ +6a_1x+2a_2+\frac{q_u}{C} \tag{33}$$

$$\frac{d^2\psi}{dx^2}=\frac{d}{dx}\left(\frac{d\psi}{dx}\right)=24a_0x+6a_1 \tag{34}$$

$$\psi=\frac{dw}{dx}+\frac{D}{C}\frac{d^2\psi}{dx^2}= \\ 4a_0x^3+3a_1x^2+2a_2x+a_3+ \\ \frac{D}{C}\left[24a_0x+6a_1\right] \tag{35}$$

The boundary conditions on the junction point with AA′ segment are as follows:

$$M\big|_{x=0}=-M_A \tag{36}$$

$$V\big|_{x=0}=V_A \tag{37}$$

$$\psi\big|_{x=0}=\psi_A \tag{38}$$

The unknown coefficients, a_1, a_2 and a_3, can be evaluated by using the above boundary conditions.

$$M\left|\begin{array}{l}x=0=-M_A\rightarrow \\ -D\dfrac{d\psi}{dx}\big|_{x=0}=-D\left(2a_2+\dfrac{q_u}{C}\right)=\end{array}\right. \\ -2\alpha\beta AD_1\rightarrow a_2=\alpha\beta A\frac{D_1}{D}-\frac{q_u}{2C} \tag{39}$$

$$V\left|\begin{array}{l}x=0=V_A\rightarrow C\left(\dfrac{dw}{dx}-\psi\right)\big|_{x=0}= \\ -D\dfrac{d^2\psi}{dx^2}\big|_{x=0}=-6Da_1\end{array}\right. = \\ AD_1\beta\left[-3\alpha^2+\beta^2+\frac{k_s}{C_1}\right] \\ \rightarrow a_1=-\frac{1}{6}A\beta\frac{D_1}{D}\left[-3\alpha^2+\beta^2+\frac{k_s}{C_1}\right] \tag{40}$$

$$\psi\Big|_{x=0}=\psi_A\rightarrow a_3+\frac{6D}{C}a_1= \\ A\beta+\frac{AD_1\beta}{C_1}\left[3\alpha^2-\beta^2-\frac{k_s}{C_1}\right] \\ \rightarrow a_3= \\ A\beta\left\{1+\left(\frac{D_1}{C}-\frac{D_1}{C_1}\right)\left[-3\alpha^2+\beta^2+\frac{k_s}{C_1}\right]\right\} \tag{41}$$

At point B, the bending moment is zero and the displacement is equal to half of the transverse component of the fault movement.

$$M\left|\begin{array}{l}x=L_c=0\rightarrow -D \\ \left[12a_0L_c^2+6a_1L_c+2a_2+\dfrac{q_u}{C}\right]=0\rightarrow A=\end{array}\right. \\ \frac{q_uL_c^2}{2\beta D_1\left[\left(-3\alpha^2+\beta^2+\dfrac{k_s}{C_1}\right)L_c-2\alpha\right]} \tag{42}$$

$$w\left|\begin{array}{l}x=L_c=\delta\rightarrow a_0L_c^4+a_1L_c^3+ \\ a_2L_c^2+a_3L_c=\end{array}\right. \\ \delta,\delta=\frac{\Delta y}{2}=\frac{\Delta f\ \sin\varphi}{2} \tag{43}$$

where Δf: is the fault movement and φ: is the fault intersection angle.

With regards to Eqs. (32), (39), (40), (41) and (42), Eq. (43) becomes a polynomial equation in terms of L_c which can be solved iteratively by the Newton–Raphson method.

$$\frac{q_u}{24D}L_c^4+\frac{\left[3\alpha^2-\beta^2-\dfrac{k_s}{C_1}\right]q_uL_c^5}{12D\left\{\left[-3\alpha^2+\beta^2+\dfrac{k_s}{C_1}\right]L_c-2\alpha\right\}}+ \\ \frac{\alpha q_uL_c^4}{2D\left\{\left[-3\alpha^2+\beta^2+\dfrac{k_s}{C_1}\right]L_c-2\alpha\right\}}+ \\ \frac{\left\{1+\left(\dfrac{D_1}{C}-\dfrac{D_1}{C_1}\right)\left[-3\alpha^2+\beta^2+\dfrac{k_s}{C_1}\right]\right\}q_uL_c^3}{2D_1\left\{\left[-3\alpha^2+\beta^2+\dfrac{k_s}{C_1}\right]L_c-2\alpha\right\}} \\ -\frac{q_u}{2C}L_c^2=\delta \tag{44}$$

After determining L_c, all other coefficients (A, a_1, a_2 and a_3) would be determined. Then the maximum bending moment developing on the pipeline is expressed as:

$$\frac{dM}{dx} = \frac{d}{dx}\left(-D\frac{d\psi}{dx}\right) = 0 \rightarrow -D \left[24a_0 x_{max} + 6a_1\right] = 0 \rightarrow x_{max} = -\frac{a_1}{4a_0} \quad (45)$$

$$M_{max} = -D\frac{d\psi}{dx}\Big|_{x=x_{max}} = -D\left[12a_0 x_{max}^2 + 6a_1 x_{max} + 2a_2 + \frac{q_u}{C}\right] \quad (46)$$

Note that according to the coordinate systems considered for segments AB and BC, q_u value is negative ($q_u = -N_{qh}\gamma H(2R)$).

Calculation of the Bending and Axial Strains

After calculating the maximum bending moment, the procedure that is used to obtain the bending and axial strains is like the procedure used in Karamitros et al. (2007). The procedure was specified in detail in Karamitros et al. (2007) and also is presented in the Appendix.

RESULTS

This study considers a refinement to the methodology presented by Karamitros et al. (2007) and the proposed model results are compared with their. Comparison between the proposed model results with the experimental results, which include a series of physical tests, and the finite element models results, which consider the shear deformations effect by using the Timoshenko beam to model pipe, is under investigation by authors. The numerical results are determined using the following data. The pipe is a gas line with properties of R = 0.4572 m and t = 0.0119 m. The characteristics of the bilinear stress-strain curve of steel pipeline are σ_1 = 490 MPa, E_1 = 210 GPa, $\varepsilon_1 = \sigma_1/E_1$ = 0.233% and E_2 = 1.088 GPa. The friction angle (ϕ) and the unit weight of the soil (γ) which are required to calculate the soil springs properties are equal to 36° and 18 KN/m^3, respectively. Also, k_0 and f are equal to 1 and 0.8, respectively.

The numerical results which cover the bending strain, the axial strain, and the maximum longitudinal strain ($\varepsilon_{max} = \varepsilon_a + \varepsilon_b$) values for the burial depth (H) ranged from 0.1 to 6 m, are presented in Figure 2. The results are computed for $\Delta f/D$ = 0.5 (Δf = 0.45 m) and three different intersection angles. As demonstrated in Figure 2, the difference between the proposed methodology results and the results of Karamitros et al. (2007) increases with increasing the burial depth. In fact, the effect of the shear deformations on the results increases versus the burial depth because the soil effect on the pipeline is more in deeper areas. It is clear that for burial depth values ranged from 1 to 3 m, the effect of the shear deformations on the results is not much remarkable but for deeper buried pipelines, the shear deformations affect the results significantly. Also, the difference between these two models for the intersection angle equal to 45° is less than the two other intersection angels. Furthermore, Figure 2 indicates that bending and axial strains decrease with considering the shear deformations by using the Timoshenko beam theory in the proposed model.

The stress-strain relationship of the steel pipeline is assumed bilinear to include the material nonlinearity (see Figure 5 in Karamitros et al. (2007)). The sudden jumps in strain indicated in Figure 2 could be related to using the bilinear stress-strain relationship for the steel material.

According to the ALA-ASCE guidelines, the peak compressive strains should be limited to 0.88 t/R. For the analyzed pipe, this limit is 0.0229, around 2.3%. The results

presented in Figure 2 show that for burial depth smaller than 5 m, the compressive strains are smaller than this limit when only the bending strains are considered (tensile axial strains are not considered in checking the peak compressive strains limitation). For burial depth higher than 5 m, the bending strains are higher than the peak compressive strains limitation and a pipe with higher resistance should be used. It should be noted that the numerical results are determined using the data presented in Karamitros et al. (2007) and the burial depth for the considered pipeline in their research was 1.3 m.

The results of these two models are presented in Tables 1 and 2 for burial depth equal to 2 m and $\Delta f/D$ equal to 0.5 and 1, respectively. Also, Tables 3 and 4 present the results for burial depth equal to 4 m and $\Delta f/D$ equal to 0.5 and 1, respectively. The results are specified in these tables to better understand the difference between the results of these two models.

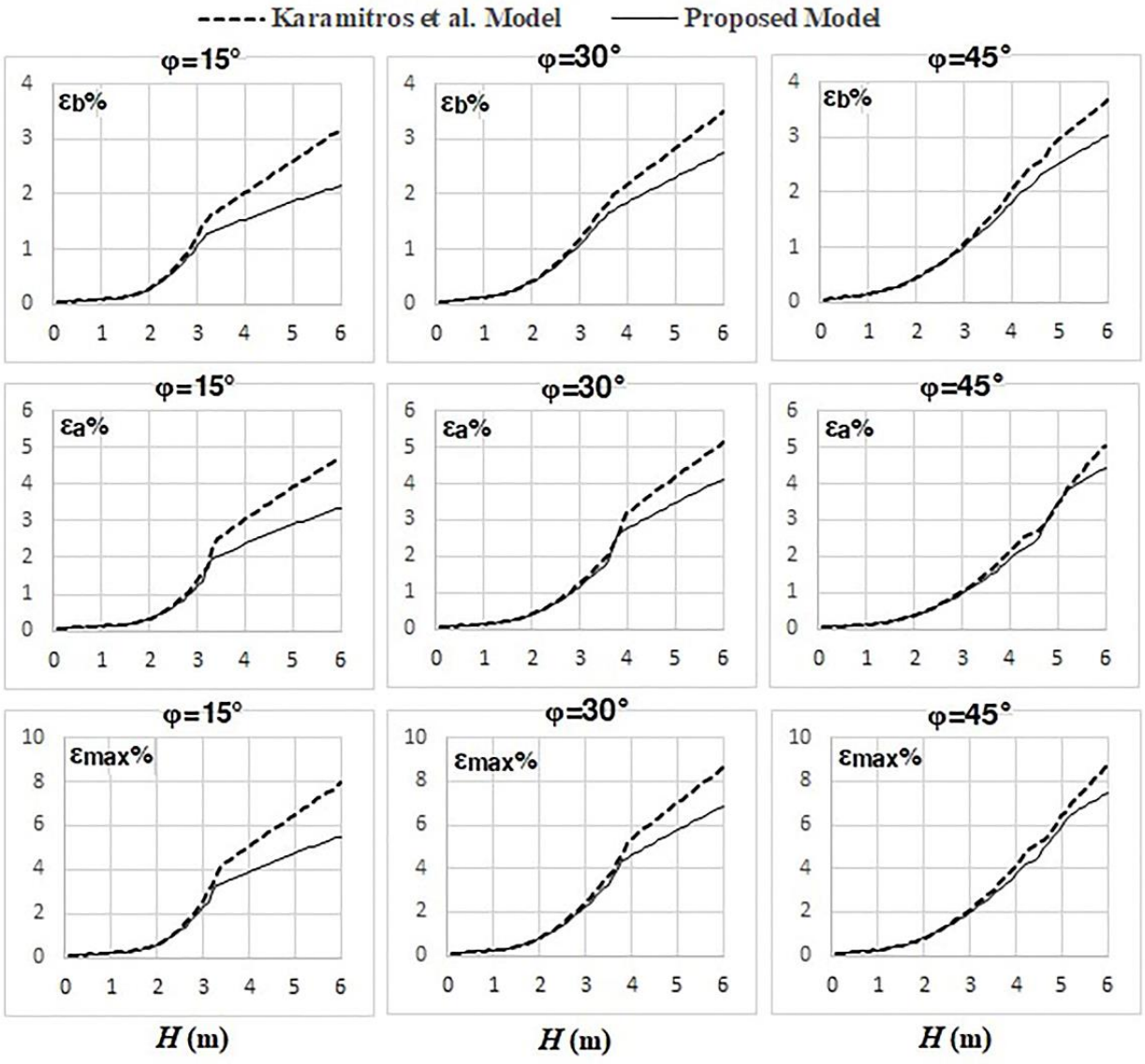

Fig. 2. Comparison of the proposed methodology results with the results of Karamitros et al. (2007)

Table 1. Comparison of results of the proposed model with Karamitros et al. (2007) for different fault crossing angles, Δf = 0.45 m and H = 2 m

Fault crossing angle	Peak axial strain (%)		Peak bending strain (%)		L_c (m)	
	Karamitros et al.	Proposed model	Karamitros et al.	Proposed model	Karamitros et al.	Proposed model
15	0.34	0.32	0.29	0.26	3.5	3.49
30	0.41	0.39	0.42	0.39	3.97	3.95
45	0.39	0.36	0.45	0.41	4.6	4.60
60	0.31	0.29	0.43	0.4	5.36	5.33
75	0.2	0.19	0.37	0.35	6.19	6.16
85	0.1	0.09	0.33	0.31	6.82	6.77

Table 2. Comparison of results of the proposed model with Karamitros et al. (2007) for different fault crossing angles, Δf = 0.9 m and H = 2 m

Fault crossing angle	Peak axial strain (%)		Peak bending strain (%)		L_c (m)	
	Karamitros et al.	Proposed model	Karamitros et al.	Proposed model	Karamitros et al.	Proposed model
15	1.8	1.8	0.9	0.84	0.7	0.67
30	1.43	1.38	0.92	0.89	0.72	0.69
45	1.08	1.05	0.93	0.9	1.53	1.49
60	0.81	0.78	0.84	0.8	3.65	3.65
75	0.55	0.52	0.73	0.69	5.55	5.53
85	0.31	0.3	0.64	0.6	6.92	6.89

Table 3. Comparison of results of the proposed model with Karamitros et al. (2007) for different fault crossing angles, Δf = 0.45 m and H = 4 m

Fault crossing angle	Peak axial strain (%)		Peak bending strain (%)		L_c (m)	
	Karamitros et al.	Proposed model	Karamitros et al.	Proposed model	Karamitros et al.	Proposed model
15	3.04	2.36	2.02	1.54	0.66	0.58
30	3.21	2.75	2.18	1.84	0.69	0.63
45	2.12	1.9	2.03	1.8	1.25	1.21
60	1.51	1.37	1.62	1.47	2.34	2.30
75	0.94	0.84	1.22	1.09	3.41	3.38
85	0.48	0.43	0.97	0.86	4.14	4.11

Table 4. Comparison of results of the proposed model with Karamitros et al. (2007) for different fault crossing angles, Δf = 0.9 m and H = 4 m

Fault crossing angle	Peak axial strain (%)		Peak bending strain (%)		L_c (m)	
	Karamitros et al.	Proposed model	Karamitros et al.	Proposed model	Karamitros et al.	Proposed model
15	4.11	4.11	2.08	1.78	0.68	0.62
30	3.75	3.75	2.17	1.98	0.69	0.66
45	3.46	3.25	2.23	2.08	0.7	0.68
60	3.42	3.25	2.29	2.17	0.72	0.69
75	1.99	1.88	2.13	2	2.38	2.35
85	1.21	1.11	1.84	1.69	3.87	3.85

Tables 1 to 4 show that the difference between the results of the present model and Karamitros et al. (2007) model is 5-10%, 0-7%, 10-24 % and 0-15 % in Tables 1 to 4, respectively. So the difference between the results of these two methods is more for higher burial depth (H = 4 m compared with H = 2 m) and smaller fault movement (Δf = 0.45 m compared with Δf = 0.9 m). The axial and bending strains obtained via the proposed

model are always smaller than the strains determined by Karamitros et al. (2007). It should be noted that the Timoshenko beam theory will predict the behavior of a beam always better than the Euler-Bernoulli beam theory. The results presented in Tables 1 to 4 show that both models predict the length of segments AB and BC (L_c) close to each other. With regard to the determined length of segments AB and BC (L_c) in Tables 1 to 4, these segments are specified as short beams in most considered cases, and therefore it is better to use the Timoshenko beam theory to predict their behavior.

CONCLUSIONS

A solution in regards to the stress-strain analysis of buried steel pipelines crossing strike-slip faults was presented by using the Timoshenko beam theory and following the general concepts employed in Karimitros et al. (2007) methodology. The difference between the proposed model results which takes into account the shear deformations and the results of the model introduced by Karamitrous et al. (2007) were considered.

Results revealed that:

- Both the axial and bending strains generally decrease by using the Timoshenko beam theory and considering the shear deformations in the proposed model.
- An increase in burial depth causes a greater difference between the results of the proposed model and the Karimitros et al. (2007) model. In fact, the effect of the shear deformations on the results increases when the burial depth increases.

REFERENCES

Abdoun, T.H., Ha, D., O'Rourke, M.J., Symans, M.D., O'Rourke, T.D., Palmer, M.C. and Stewart, H.E. (2009). "Factors influencing the behavior of buried pipelines subjected to earthquake faulting", *Soil Dynamics and Earthquake Engineering*, 29(3), 415-427.

ALA (American Lifeline Alliance). (2001). *Guidelines for the design of buried steel pipe*, FEMA, Washington, DC.

Barros, R.C. and Pereira, M. (2004). "A parametric study on the comprehensive analysis of pipelines under generalized actions", *13th World Conference on Earthquake Engineering*, Vancouver, B.C., Canada.

Chaudhari, V., Kumar, V.D. and Kumar, R.P. (2013). "Finite Element analysis of buried continuous pipeline subjected to fault motion", *International Journal of Structural Engineering*, 4(4), 314-331.

Demofonti, G., Ferino, J., Karamanos, S.A., Vazouras, P. and Dakoulas, P. (2013). "An integrated experimental - numerical approach to predict strain demand for buried steel pipelines in geo-hazardous areas", *Rio Pipeline Conference and Exposition*, Rio de Janeiro, Brazil.

Erami, M.H., Miyajima, M., Kaneko, S., Toshima, T. and Kishi, S. (2015). "Pipe-soil interaction for segmented buried pipelines subjected to dip faults", *Earthquake Engineering and Structural Dynamics*, 44(3), 403-417.

Ha, D., Abdoun, T.H., O'Rourke, M.J., Symans, M.D., O'Rourke, T.D., Palmer, M.C. and Stewart, H.E. (2010). "Earthquake faulting effects on buried pipelines – case history and centrifuge study", *Journal of Earthquake Engineering*, 14(5), 646-669.

Hojat Jalali, H., Rofooei, F.R. and Attari, N.K.A. (2018). "Performance of buried gas distribution pipelines subjected to reverse fault movement", *Journal of Earthquake Engineering*, 22(6), 1068-1091.

Hojat Jalali, H., Rofooei, F.R., Attari, N.K.A. and Samadian, M. (2016). "Experimental and finite element study of the reverse faulting effects on buried continuous steel gas pipelines", *Soil Dynamics and Earthquake Engineering*, 86, 1-14.

Hutchinson, J.R. (2001). "Shear coefficients for Timoshenko beam theory", *Journal of Applied Mechanics*, 68, 87-92.

Karamitros, D.K., Bouckovalas, G.D. and Kouretzis, G.P. (2007). "Stress analysis of buried steel pipelines at strike-slip fault crossings", *Soil Dynamics and Earthquake Engineering*, 27(3), 200-211.

Kennedy, R.P., Chow, A.W. and Williamson, R.A. (1977). "Fault movement effects on buried oil pipeline", *Transportation Engineering Journal of ASCE*, 103(5), 617-633.

Moradi, M., Rojhani, M., Ghalandarzadeh, A. and Takada, S. (2013). "Centrifuge modeling of buried continuous pipelines subjected to normal faulting", *Earthquake Engineering and Engineering Vibration*, 12(1), 155-164.

Newmark, N.M. and Hall, W.J. (1975). "Pipeline

design to resist large fault displacement", *Proceedings of the U.S. National Conference on Earthquake Engineering*, Ann Arbor: University of Michigan.

O'Rourke, M.J. and Liu, X. (2012). *Seismic design of buried and offshore pipelines*, Monograph MCEER-12-MN04, The Multidisciplinary Center for Earthquake Engineering Research, Buffalo, New York.

O'Rourke, T.D. and Palmer, M.C. (1996). "Earthquake performance of gas transmission pipelines", *Earthquake Spectra*, 12(3), 493-527.

Rashidifar, M.A. and Rashidifar, A.A. (2013). "Analysis of vibration of a pipeline supported on elastic soil using differential transform method", *American Journal of Mechanical Engineering*, 1(4), 96-102.

Saiyar, M., Ni, P., Take, W.A. and Moore, I.D. (2016). "Response of pipelines of different flexural stiffness to normal faulting", *Géotechnique*, 66(4), 275-286.

Sarvanis, G.C. and Karamanos, S.A. (2017). "Analytical model for the strain analysis of continuous buried pipelines in geohazard", *Engineering Structures*, 152, 57-69.

Sarvanis, G.C., Karamanos, S.A., Vazouras, P., Mecozzi, E., Lucci, A. and Dakoulas, P. (2017). "Permanent earthquake-induced actions in buried pipelines: Numerical modeling and experimental verification", *Earthquake Engineering and Structural Dynamics*, 47(4), 1-22.

Takada, S., Hassani, N. and Fukuda, K. (2001). "A new proposal for simplified design of buried steel pipes crossing active faults", *Earthquake Engineering and Structural Dynamics*, 30(8), 1243-1257.

Timoshenko, S.P. (1921). "On the correction shear of shear of the differential equation for transverse vibration of prismatic bars", *Philosophical Magazine*, 41, 744-746.

Towhata, I. (2010). *Geotechnical earthquake engineering*, Springer Series in Geo-Mechanics and Geoengineering, pp. 684.

Trifonov, O.V. (2015). "Numerical stress-strain analysis of buried steel pipelines crossing active strike-slip faults with an emphasis on fault modeling aspects", *Journal of Pipeline Systems Engineering and Practice*, 6(1), 04014008-1-04014008-10.

Trifonov, O.V. and Cherniy, V.P. (2010). "A semi-analytical approach to a nonlinear stress-strain analysis of buried steel pipelines crossing active faults", *Soil Dynamics and Earthquake Engineering*, 30(11), 1298-1308.

Uckan, E., Akbas, B., Shen, J., Rou, W., Paolacci, F. and O'Rourke, M. (2015). "A simplified analysis model for determining the seismic response of buried steel pipes at strike-slip fault crossings", *Soil Dynamics and Earthquake Engineering*, 75, 55-65.

Van ES, S.H.J. and Gresnigt, A.M. (2016). "Experimental and numerical investigation into the behavior of buried steel pipelines under strike-slip fault movement", *Proceedings of the 11th International Pipeline Conference*, Calgary, Alberta, Canada.

Vazouras, P., Dakoulas, P. and Karamanos, S.A. (2015). "Pile-soil interaction and pipeline performance under strike-slip fault movements", *Soil Dynamics and Earthquake Engineering*, 72, 48-65.

Wang, L.R.L. and Yeh, Y.A. (1985). "A refined seismic analysis and design of buried pipeline for fault movement", *Earthquake Engineering and Structural Dynamics*, 13(1), 75-96.

Xie, X., Symans, M.D., O'Rourke, M.J., Abdoun, T.H., O'Rourke, T.D., Palmer, M.C. and Stewart, H.E. (2011). "Numerical modeling of buried HDPE pipelines subjected to strike-slip faulting", *Journal of Earthquake Engineering*, 15(8), 1273-1296.

Xie, X., Symans, M.D., O'Rourke, M.J., Abdoun, T.H., O'Rourke, T.D., Palmer, M.C. and Stewart, H.E. (2013). "Numerical modeling of buried HDPE pipelines subjected to normal faulting: A case study", *Earthquake Spectra*, 29(2), 609-632.

Yin, J.H. (2000). "Closed-form solution for reinforced Timoshenko beam on elastic foundation", *Journal of Engineering Mechanics*, 126(8), 868-874.

Zhang, L., Liang, Z. and Han, C.J. (2014). "Buckling behavior analysis of buried gas pipeline under strike-slip fault displacement", *Journal of Natural Gas Science and Engineering*, 21, 921-928.

Zhang, L., Zhao, X., Yan, X. and Yang, X. (2016). "A new finite element model of buried steel pipelines crossing strike-slip faults considering equivalent boundary springs", *Engineering Structures*, 123, 30-44.

APPENDIX

Reaching Eq. (6) from Eqs. (1) and (2):

Eqs. (1) and (2) were expressed as:

$$D_1 \frac{d^2\psi}{dx^2} - C_1\psi + C_1 \frac{dw}{dx} = 0 \qquad \text{(A - 1)}$$

$$C_1 \frac{d\psi}{dx} - C_1 \frac{d^2w}{dx^2} + k_s w = 0 \qquad \text{(A - 2)}$$

Differentiation of Eq. (A.1) yields:

$$D_1 \frac{d^3\psi}{dx^3} - C_1 \frac{d\psi}{dx} + C_1 \frac{d^2w}{dx^2} = 0 \qquad \text{(A - 3)}$$

Using Eq. (A.2) and Eq. (A.3) yields:

$$D_1 \frac{d^3\psi}{dx^3} + k_s w = 0 \qquad \text{(A - 4)}$$

Also, using Eq. (A.2) yields:

$$\frac{d\psi}{dx} = \frac{d^2w}{dx^2} - \frac{k_s}{C_1} w \qquad \text{(A - 5)}$$

Double differentiation of Eq. (A.5) yields:

$$\frac{d^3\psi}{dx^3} = \frac{d^4w}{dx^4} - \frac{k_s}{C_1} \frac{d^2w}{dx^2} \qquad \text{(A - 6)}$$

Using Eq. (A.4) and Eq. (A.6) yields:

$$D_1 \frac{d^4w}{dx^4} - \frac{k_s D_1}{C_1} \frac{d^2w}{dx^2} + k_s w = 0 \qquad \text{(A - 7)}$$

Reaching Eq. (28) from Eqs. (24) and (25):

Eqs. (24) and (25) were expressed as:

$$D \frac{d^2\psi}{dx^2} - C\psi + C \frac{dw}{dx} = 0 \qquad \text{(A - 8)}$$

$$C \frac{d\psi}{dx} - C \frac{d^2w}{dx^2} = q \qquad \text{(A - 9)}$$

Differentiation of Eq. (A.8) yields:

$$D \frac{d^3\psi}{dx^3} - C \frac{d\psi}{dx} + C \frac{d^2w}{dx^2} = 0 \qquad \text{(A - 10)}$$

Using Eq. (A.9) and Eq. (A.10) yields:

$$D \frac{d^3\psi}{dx^3} = q \qquad \text{(A - 11)}$$

Also, using Eq. (A.9) yields:

$$\frac{d\psi}{dx} = \frac{d^2w}{dx^2} + \frac{q}{C} \qquad \text{(A - 12)}$$

Double differentiation of Eq. (A.12) yields:

$$\frac{d^3\psi}{dx^3} = \frac{d^4w}{dx^4} + \frac{d^2q}{Cdx^2} \qquad \text{(A - 13)}$$

Using Eq. (A.11) and Eq. (A.13) yields:

$$D \frac{d^4w}{dx^4} = q - \frac{D}{C} \frac{d^2q}{dx^2} \qquad \text{(A - 14)}$$

Calculation of the Bending and Axial Strains

The bending strains can be evaluated as:

$$\varepsilon_b^{I} = \frac{M_{max} R}{EI} \qquad \text{(A - 15)}$$

Geometrical second order effects are not taking into account in Eq. (A.15). According to Karamitros et al. (2007), the actual bending strain is expressed as:

$$\frac{1}{\varepsilon_b} = \frac{1}{\varepsilon_b^{I}} + \frac{1}{\varepsilon_b^{II}} \qquad \text{(A - 16)}$$

where ε_b^{II}: is the bending strains calculated geometrically by neglecting the bending stiffness of pipeline and is given by (Karamitros et al., 2007):

$$\varepsilon_b^{II} = \frac{q_u R}{F_a} \qquad \text{(A - 17)}$$

where F_a: is the axial force at the intersection of the pipeline with the fault trace. The combination that is used in Eq. (A.16), provides a rather good approximation to real strains although it lacks physical meaning (Trifonov and Cherniy, 2010).

The axial force at the intersection of the pipeline with the fault trace is given by:

$$F_a = \sigma_a A_s \qquad \text{(A - 18)}$$

where σ_a: is the axial stress developing at the intersection point and is calculated by Karamitros et al. (2007) as:

$$\sigma_a = \begin{cases} \sqrt{\dfrac{E_1 t_u \Delta L_{req}}{A_s}} & \text{if } \Delta L_{req} \le \dfrac{\sigma_1^2 A_s}{E_1 t_u} \\ \sigma_a = \dfrac{\sigma_1 (E_1 - E_2) + \sqrt{\sigma_1^2 (E_2^2 - E_1 E_2) + E_1^2 E_2 \Delta L_{req} \dfrac{t_u}{A_s}}}{E_1} & \text{if } \Delta L_{req} \succ \dfrac{\sigma_1^2 A_s}{E_1 t_u} \end{cases} \qquad \text{(A - 19)}$$

where ΔL_{req}: is the geometrically required elongation that is defined as the elongation provoked in the pipeline by the fault movement, σ_1 and E_2: are the yield stress and the plastic Young's modulus of the pipeline steel and t_u: is the maximum axial soil force per unit length of the pipe that is defined in cohesionless soil (sand) as (ALA-ASCE, 2001):

$$t_u = \pi R \gamma H \left(1 + k_0\right) \tan\left(f\ \phi\right) \qquad \text{(A - 20)}$$

where k_0: is the coefficient of pressure at rest, f: is the coating dependent factor relating the internal friction angle of the soil to the friction angle at the soil-pipe interface and ϕ: is the internal friction angle of the soil.

According to Karamitros et al. (2007), the elongation generated due to the vertical fault displacement component Δy can be ignored compared to the elongation due to the horizontal fault displacement component Δx.

$$\Delta L_{req} = \Delta x, \Delta x = \Delta f\ \cos\varphi \qquad \text{(A - 21)}$$

$$\phi_{1,2} = \begin{cases} \pi, & \dfrac{\varepsilon_1 \mp \varepsilon_a}{\varepsilon_b} \prec -1, \\ \arccos\left(\dfrac{\varepsilon_1 \mp \varepsilon_a}{\varepsilon_b}\right), & -1 \le \dfrac{\varepsilon_1 \mp \varepsilon_a}{\varepsilon_b} \le 1, \\ 0, & 1 \prec \dfrac{\varepsilon_1 \mp \varepsilon_a}{\varepsilon_b}. \end{cases} \qquad \text{(A - 23)}$$

Eq. (A.19) is obtained by equating the geometrically required and the stress-induced pipeline elongation and assuming a bilinear stress-strain relationship for the pipeline steel (see Figure 5 in Karamitros et al. (2007)).

Calculation of the Axial Strain

As mentioned in Trifonov and Cherniy (2010), by following the developments of Karamitros and his colleagues (2007), the distribution of stresses on the cross-section (see Figure 8 in Karamitros et al. (2007)) is given by:

$$\sigma = \begin{cases} \sigma_1 + E_2(\varepsilon - \varepsilon_1), & 0 \le \theta \prec \phi_1, \\ E_1 \varepsilon, & \phi_1 \le \theta \le \pi - \phi_2, \\ -\sigma_1 + E_2(\varepsilon + \varepsilon_1), & \pi - \phi_2 \prec \theta \le \pi. \end{cases} \qquad \text{(A - 22)}$$

where ε_1: is the yield strain, θ: is the polar angle of the cross-section and the angles $\phi_{1,2}$: stand for the portion the cross-section that is under yield:

The axial force and bending moment in the cross-section are evaluated by integrating the stresses over the cross-section (Karamitros et al., 2007):

$$F = 2\int_0^{\pi} \sigma R_{\mathrm{m}} t \mathrm{d}\theta$$
$$\Rightarrow F = 2R_{\mathrm{m}} t \left[E_1 \pi \varepsilon_{\mathrm{a}} - (E_1 - E_2)(\phi_1 + \phi_2)\varepsilon_{\mathrm{a}} + (E_1 - E_2)(\phi_1 - \phi_2)\varepsilon_1 - (E_1 - E_2)(\sin\phi_1 - \sin\phi_2)\varepsilon_{\mathrm{b}}\right] \quad \text{(A - 24)}$$

$$M = 2\int_0^{\pi} \sigma R_{\mathrm{m}} t R_{\mathrm{m}} \cos\theta \mathrm{d}\theta$$
$$\Rightarrow M = 2R_{\mathrm{m}}^2 t \left[\frac{E_1 \pi \varepsilon_{\mathrm{b}}}{2} - (E_1 - E_2)(\sin\phi_1 - \sin\phi_2)\varepsilon_{\mathrm{a}} + (E_1 - E_2)(\sin\phi_1 - \sin\phi_2)\varepsilon_1 \right. \quad \text{(A - 25)}$$
$$\left. - \frac{(E_1 - E_2)(\phi_1 + \phi_2)\varepsilon_{\mathrm{b}}}{2} - \frac{(E_1 - E_2)(\sin 2\phi_1 + \sin 2\phi_2)\varepsilon_{\mathrm{b}}}{4}\right]$$

and

$$R_{\mathrm{m}} = \frac{2R - t}{2} \quad \text{(A - 26)}$$

where t: is the pipeline thickness.

The axial strain in the cross-section can be computed by equating the axial force obtaining from the integration over the cross-section to the applied axial force calculated using Eq. (A.18). The solution of Eq. (A.23) together with Eq. (A.24) results in a complex formula for ε_{a} which can be solved iteratively, using the Newton-Raphson method. Details of application of the Newton–Raphson method are given in Karamitros et al. (2007).

The computation of the maximum bending moment by Eq. (46) was based on the elastic Timoshenko beam theory and the nonlinearity behavior of steel pipeline was not taking into account. According to Karamitros et al. (2007), one can use an iterative solution by readjusting the secant Young's modulus of the pipeline steel on each iterative to consider the steel pipeline nonlinearity. If the bending moment in the cross-section that was evaluated by Eq. (A.25) is not equal to the bending moment calculated by Eq. (46), the secant modulus for the next iteration can be calculated as:

$$E_{\mathrm{sec}} = \frac{M\left(\varepsilon_{\mathrm{a}}, \varepsilon_{\mathrm{b}}\right) D}{2I\,\varepsilon_{\mathrm{b}}^{\mathrm{I}}} = \frac{M\left(\varepsilon_{\mathrm{a}}, \varepsilon_{\mathrm{b}}\right) D}{2I}\left(\frac{1}{\varepsilon_{\mathrm{b}}} - \frac{1}{\varepsilon_{\mathrm{b}}^{\mathrm{II}}}\right) \quad \text{(A - 27)}$$

Then the procedure for segments AB and BC would be repeated using the secant modulus until convergence is achieved.